Joint Multi-User Precoding in Multi-Relay Systems

Hang Long[1], Wei Xiang[2], Yueying Zhang[1], Jing Wang[1], and Wenbo Wang[1]
[1]: Key Laboratory of Universal Wireless Communication, Ministry of Education
Beijing University of Posts & Telecommunications
Beijing 100876 China
[2]: Faculty of Engineering and Surveying
University of Southern Queensland
Toowoomba, QLD 4350, Australia

***Abstract*—Multi-user precoding in multi-relay systems is investigated in this paper. Firstly, a distributed precoder through the relay nodes is presented, which performs as a sub-optimum solution in terms of both the outage probability and ergodic capacity. Then, a multi-user precoder at the source node is jointly designed, where is used to enhance the *maximum* signal-to-leakage-and-noise ratio of each data stream.**

I. Introduction

The relay technique has attracted significant attention in both academia and industry areas. Meanwhile, the multi-user (MU)-multi-input-multi-output (MIMO) system is an important research area that allows for spatial division multi-access and multi-user diversity. If only one relay node with multiple antennas is used between the source node and multiple users, the relay system can be treated as a simple concatenation of a single-user MIMO system (the source-relay link) and a MU-MIMO system (the relay-users links), where precoding schemes in conventional MIMO systems can be directly used [1], [2]. If multiple relay nodes are located between the source node and users, coherent combination of signals from multiple relay nodes and inter-stream interference (ISI) mitigation techniques are both required for the precoding design.

Similar to the work on conventional MU-MIMO systems, the downlink multi-user multi-relay systems [3] - [8] are much more popular than their uplink counterparts [9]. Precoding can be utilized at the source node to mitigate ISI [6] - [8]. On the other hand, if multiple relay nodes transmit to the users simultaneously, a distributed precoder can be used through these relay nodes. The two precoders in the downlink multi-user multi-relay system can be designed either independently or jointly.

The decode-and-forward protocol in [3] - [6] divides the entire source-relay-destination transmission into two independent parts. Additionally, the entire transmission is carried out in three phases as shown in [3] - [6], which is inefficient. Hence, precoding design for two-phase relaying protocols [7] - [9] is more attractive.

In [7], a single antenna is assumed for relay and destination nodes, where multi-user precoding at the source node and distributed precoding through relay nodes are employed. The transmit powers of the source and relay nodes are used as the optimization objective functions. However, the scheme in [7], [9] is so complicated that there is no closed-form expression for the precoder, and iterative algorithms are adopted. Similar problem exists in the design in [8], where a separate transmit power constraint for each relay node is also assumed.

With the amplify-and-forward (AF) relaying protocol, the multi-user precoder at the source node and the distributed precoder through relay nodes impact on each other. In this paper, the distributed precoder through relay nodes are designed independently at first. Considering the trade-off among multiple users, a hybrid signal-to-interference-and-noise ratio (SINR) is defined as the optimization objective function for the distributed precoder design. Then, joint precoder design of the two precoders is investigated. Users are adaptively divided into two groups. The precoding vectors at the source node of the first group are used to maximize the *maximum* signal-to-leakage-and-noise ratio (SLNR) which is defined according to the equivalent channels through relay nodes for the distributed precoder design. The precoding vectors of the second group are designed to change the equivalent channels, so that the distributed precoder can improve on the SINR of each destination node simultaneously.

II. System Model and Linear Two-phase Relaying Protocol

Notations:

$\mathbf{A}^T$, $\mathbf{A}^*$, $\mathbf{A}^H$, $\mathbf{A}^{-1}$ and $\|\mathbf{A}\|_F$ denote the transpose, conjugation, conjugate-transpose, pseudoinverse and Frobenius norm of matrix $\mathbf{A}$, respectively. $\mathbf{A}(i,j)$ is the element in the ith row and the jth column of $\mathbf{A}$. $\mathbf{A}(i,:)$ and $\mathbf{A}(:,i)$ denote the ith row and the ith column of $\mathbf{A}$, respectively. $\mathbf{I}_n$ is the $n \times n$ identity matrix. $\mathbf{0}_{m,n}$ is the $m \times n$ all-zero matrix. $\mathrm{diag}(\mathbf{a})$ is the $n \times n$ diagonal matrix with $\mathbf{a}$ as its diagonal when $\mathbf{a}$ is an $n \times 1$ or $1 \times n$ vector. $\mathcal{E}(\cdot)$ represents mathematical expectation. $\Pr(\cdot)$ is used as the probability notation. $\lfloor x \rfloor$ is the largest integer which is not larger than x.

Fig. 1 illustrates the multi-user multi-relay system under consideration in this study, which is comprised of one source node (S), N_R relay nodes ($R_i,\ i \in \{1,2,\cdots,N_R\}$) and N_D destination nodes ($D_j,\ j \in \{1,2,\cdots,N_D\}$). N_S antennas are equipped at S, whereas a single antenna is assumed for the other nodes. Direct links between the source and

[0]This research was supported by the National Science Foundation for Post-doctoral Scientists of China under Grant 20110490329 and National Key Technology R&D Program of China under Grant 2010ZX03005-001-03.

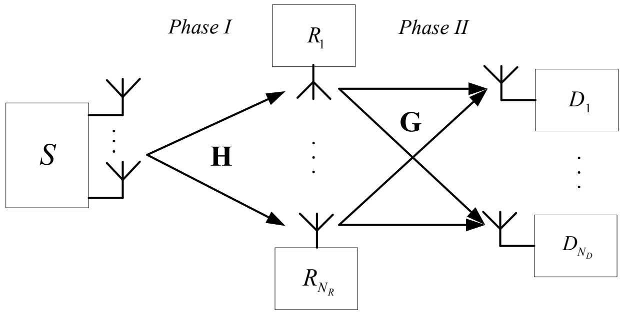

Fig. 1. System model of the multi-user multi-relay system.

destination nodes are not considered in this study. Without explicit explanation, i is used as the index of a relay node ($i \in \{1, 2, \cdots, N_R\}$), and j is used as the index of a destination node ($j \in \{1, 2, \cdots, N_D\}$) in the following.

In *Phase I*, the transmit signal of S is $\mathbf{x}_S \in \mathbb{C}^{N_S \times 1}$ with the power constraint of $\mathcal{E}(\mathbf{x}_S^H \mathbf{x}_S) = E_S$, and the received signal at R_i is y_{R_i}. The received signals at N_R relay nodes can be written in vector form

$$\underbrace{\begin{bmatrix} y_{R_1} \\ \vdots \\ y_{R_{N_R}} \end{bmatrix}}_{\mathbf{y}_R} = \underbrace{\begin{bmatrix} h_{1,1} & \cdots & h_{1,N_S} \\ \vdots & \ddots & \vdots \\ h_{N_R,1} & \cdots & h_{N_R,N_S} \end{bmatrix}}_{\mathbf{H}} \mathbf{x}_S + \underbrace{\begin{bmatrix} n_{R_1} \\ \vdots \\ n_{R_{N_R}} \end{bmatrix}}_{\mathbf{n}_R}. \quad (1)$$

In *Phase II*, the relaying signal of R_i is x_{R_i}, and the received signal at D_j is y_{D_j}. Similarly, the received signals at N_D destination nodes can also be written in vector form

$$\underbrace{\begin{bmatrix} y_{D_1} \\ \vdots \\ y_{D_{N_D}} \end{bmatrix}}_{\mathbf{y}_D} = \underbrace{\begin{bmatrix} g_{1,1} & \cdots & g_{1,N_R} \\ \vdots & \ddots & \vdots \\ g_{N_D,1} & \cdots & g_{N_D,N_R} \end{bmatrix}}_{\mathbf{G}} \underbrace{\begin{bmatrix} x_{R_1} \\ \vdots \\ x_{R_{N_R}} \end{bmatrix}}_{\mathbf{x}_R} + \underbrace{\begin{bmatrix} n_{D_1} \\ \vdots \\ n_{D_{N_D}} \end{bmatrix}}_{\mathbf{n}_D}. \quad (2)$$

In (1) and (2), $i \in \{1, 2, \cdots, N_R\}$, $j \in \{1, 2, \cdots, N_D\}$, and $k \in \{1, 2, \cdots, N_S\}$. In addition,

- $h_{i,k}$ is the channel gain from the kth antenna of S to R_i;
- $g_{j,i}$ is the channel gain from R_i to D_j;
- n_{R_i} and n_{D_j} denote the additive white Gaussian noise at R_i and D_j, respectively, i.e., $n_{R_i}, n_{D_j} \sim \mathcal{CN}(0, \sigma^2)$.

Noted that the two-phase relaying protocol assumed in this study is different from those in [3] - [6]. In *Phase I*, the transmit signal of S can be rewritten as

$$\mathbf{x}_S = \mathbf{F}\mathbf{d} \quad (3)$$

where $\mathbf{d} \in \mathbb{C}^{N_D \times 1}$ is the data vector before precoding, and $\mathbf{F}$ is the precoding matrix at S. It is assumed that only one data stream is sent to each destination node, so that $\mathcal{E}(\mathbf{d}\mathbf{d}^H) = \mathbf{I}_{N_D}$. $\mathbf{F}$ is constrained as $\|\mathbf{F}\|_F^2 = E_S$ to satisfy the power constraint of S. It is assumed that $N_S \geq N_D$ and $N_R \geq N_D$.

In *Phase II*, the transmit signal of R_i can be written as a linear function of the received signal

$$x_{R_i} = \beta_i y_{R_i} \quad (4)$$

with β_i being the relaying coefficient of R_i. We can divide β_i into two parts as follows

$$\beta_i = p_i \alpha_i \quad (5)$$

where α_i is the power normalization coefficient with $\alpha_i^2 \mathcal{E}[|y_{R_i}|^2] = 1$. Integrating (3) into (1) gives rise to

$$\alpha_i^{-2} = \mathcal{E}[|y_{R_i}|^2] = \|\mathbf{H}(i,:)\mathbf{F}\|_F^2 + \sigma^2, i \in \{1, 2, \cdots, N_R\}. \quad (6)$$

In (5), p_i is the distributed precoding element of R_i. The distributed precoding elements of the N_R relay nodes constitute the distributed precoding vector $\mathbf{p} = [p_1, p_2, \cdots, p_{N_R}]^T$. The relaying signal vector $\mathbf{x}_R$ can also be written as a linear function of $\mathbf{y}_R$

$$\mathbf{x}_R = \mathbf{B}\mathbf{y}_R \quad (7)$$

where

$$\mathbf{B} = \mathrm{diag}(\mathbf{a})\mathrm{diag}(\mathbf{p}) \quad (8)$$

is the diagonal relaying matrix, and

$$\mathbf{a} = [\alpha_1, \alpha_2, \cdots, \alpha_{N_R}]^T \quad (9)$$

is the normalization vector.

Integrating (1), (3) and (7) into (2) gives

$$\mathbf{y}_D = \mathbf{GBHFd} + \mathbf{GB}\mathbf{n}_R + \mathbf{n}_D. \quad (10)$$

We can define the equivalent channel matrix as

$$\mathbf{H}^{(e)} = \mathbf{GBHF}. \quad (11)$$

The diagonal elements of $\mathbf{H}^{(e)}$ are the equivalent channels of the target signals at the destination nodes, whereas the other elements of $\mathbf{H}^{(e)}$ represent ISI. Therefore, ISI cannot be suppressed at the receiver since only a single antenna is equipped at each destination node.

The covariance matrix of the equivalent noise is defined as

$$\begin{aligned} \mathbf{R}_n &= \mathcal{E}[(\mathbf{GB}\mathbf{n}_R + \mathbf{n}_D)(\mathbf{GB}\mathbf{n}_R + \mathbf{n}_D)^H] \\ &= (\mathbf{GBB}^H\mathbf{G}^H + \mathbf{I}_{N_D})\sigma^2. \end{aligned} \quad (12)$$

According to (10)-(12), the received SINR at D_j can be calculated as

$$\gamma_j = \frac{\left|\mathbf{H}^{(e)}(j,j)\right|^2}{\left\|\mathbf{H}^{(e)}(j,:)\right\|_F^2 - \left|\mathbf{H}^{(e)}(j,j)\right|^2 + \mathbf{R}_n(j,j)} \quad (13)$$

where $j \in \{1, 2, \cdots, N_D\}$.

As can be seen in (11), the equivalent channel matrix $\mathbf{H}^{(e)}$ is a function of $\mathbf{F}$ and $\mathbf{B}$ ($\mathbf{p}$). On the other hand, $\mathbf{R}_n$ is also affected by $\mathbf{B}(\mathbf{p})$. The multi-user precoding matrix $\mathbf{F}$ and the distributed precoding vector $\mathbf{p}$ should be carefully designed to mitigate ISI and ensure coherent combination of signals from multiple relay nodes.

III. Distributed Precoding through Relay Nodes

In this section, distributed precoding design is studied without considering the multi-user precoding matrix $\mathbf{F}$, i.e., $N_S = N_D$, and $\mathbf{F} = \mathbf{I}_{N_D}$. Under this assumption, the distributed precoder $\mathbf{p}$ has two effects: 1) coherent combination of signals from N_R relay nodes at each destination node; 2) ISI mitigation. Additionally, the trade-off among the N_D destination nodes should also be considered in the distributed precoder design.

The normalized channel matrix of *Phase II* is defined as

$$\mathbf{G}_a = \mathbf{G}\mathrm{diag}(\mathbf{a}). \tag{14}$$

The equivalent channel vector of target signal d_j from S to D_j through N_R relay nodes is defined as

$$\mathbf{e}_j = \mathrm{diag}\left[\mathbf{G}_a\left(j,:\right)\right]\mathbf{H}\left(:,j\right), j \in \{1,2,\cdots,N_D\}. \tag{15}$$

Correspondingly, the power of the received target signal at D_j is $|\mathbf{H}^{(e)}(j,j)|^2 = \mathbf{p}^T\mathbf{e}_j\mathbf{e}_j^H\mathbf{p}^*$. Likewise, the interference channel vector of d_k at D_j ($k \neq j$) is defined as

$$\mathbf{c}_{kj} = \mathrm{diag}\left[\mathbf{G}_a\left(j,:\right)\right]\mathbf{H}\left(:,k\right), j,k \in \{1,2,\cdots,N_D\}. \tag{16}$$

$|\mathbf{H}^{(e)}(j,k)|^2 = \mathbf{p}^T\mathbf{c}_{kj}\mathbf{c}_{kj}^H\mathbf{p}^*$ is the received interference power at D_j from d_k, i.e., the data stream for the kth user.

The received relaying noise power at D_j is $\mathbf{p}^T\mathbf{R}_{D_j}\mathbf{p}^*\sigma^2$, in which

$$\mathbf{R}_{D_j} = \mathrm{diag}\left\{\left[\left|\mathbf{G}_a\left(j,1\right)\right|^2, \left|\mathbf{G}_a\left(j,2\right)\right|^2, \cdots, \left|\mathbf{G}_a\left(j,N_R\right)\right|^2\right]\right\}. \tag{17}$$

The received SINR of D_j in (13) is rewritten as a function of $\mathbf{p}$

$$\gamma_j = \frac{\mathbf{p}^T\mathbf{e}_j\mathbf{e}_j^H\mathbf{p}^*}{\mathbf{p}^T\left[\sum\limits_{k,k\neq j}(\mathbf{c}_{kj}\mathbf{c}_{kj}^H) + \mathbf{R}_{D_j}\sigma^2\right]\mathbf{p}^* + \sigma^2}. \tag{18}$$

In this section, the total power of N_R relay nodes is constrained as $\mathcal{E}(\mathbf{x}_R^H\mathbf{x}_R) = E_R$, which is different from the assumption in [8]. Since α_i is used to normalize the power of the received signal at each relay node, the total power constraint of the relay nodes is equivalent to the Frobenius norm of the precoding vector $\mathbf{p}$

$$\|\mathbf{p}\|_F^2 = \mathbf{p}^T\mathbf{I}_{N_R}\mathbf{p}^* = E_R. \tag{19}$$

According to (19), the last term in the denominator of (18) can be rewritten as $\sigma^2 = \mathbf{p}^T(\sigma^2/E_R\mathbf{I}_{N_R})\mathbf{p}^*$. As a result, (18) is rewritten as

$$\gamma_j = \frac{\mathbf{p}^T\mathbf{e}_j\mathbf{e}_j^H\mathbf{p}^*}{\mathbf{p}^T\mathbf{C}_j\mathbf{p}^*} \tag{20}$$

where

$$\mathbf{C}_j = \sum_{k,k\neq j}\mathbf{c}_{kj}\mathbf{c}_{kj}^H + \left(\mathbf{R}_{D_j} + \frac{1}{E_R}\mathbf{I}_{N_R}\right)\sigma^2. \tag{21}$$

The optimization objective function is fairly important in the precoder design. Objective functions in relation to system capacity and reliability are usually adopted, e.g.,

$$\mathbf{p}_{\mathrm{MC}} = \underset{\|\mathbf{p}\|_F^2 = E_R}{\arg\max}\sum_{j=1}^{N_D}\log_2\left(1+\gamma_j\right) \tag{22}$$

and

$$\mathbf{p}_{\mathrm{MM}} = \underset{\|\mathbf{p}\|_F^2 = E_R}{\arg\max}\left(\min_{1\leq j\leq N_D}\gamma_j\right). \tag{23}$$

The precoder design in (22) can achieve the maximum system capacity performance, whereas the one in (23) with maximizing the minimum SINR is usually employed for the system reliability performance improvement.

Generally speaking, system capacity and reliability are two conflicting design criteria in multi-user systems. A precoder design cannot perform well in both criteria. A trade-off between reliability and capacity performance needs to be considered. Also, the trade-off among the N_D users should be taken into account. Therefore, a hybrid SINR is proposed as follows

$$\gamma_E = \frac{\mathbf{p}^T\mathbf{E}\mathbf{p}^*}{\mathbf{p}^T\mathbf{C}\mathbf{p}^*} \tag{24}$$

where

$$\mathbf{E} = \sum_{j=1}^{N_D}(\mathbf{e}_j\mathbf{e}_j^H), \mathbf{C} = \sum_{j=1}^{N_D}\mathbf{C}_j. \tag{25}$$

The numerator of γ_E is the sum of the numerators of $\gamma_j, j \in \{1,2,\cdots,N_D\}$, whose denominators are added to become the denominator of γ_E. The precoder is achieved as follows

$$\mathbf{p}_H = \underset{\|\mathbf{p}\|_F^2 = E_R}{\arg\max}\,\gamma_E. \tag{26}$$

The received powers of the N_D users are equally combined in the expression of γ_E, whereas the interference covariance matrices are also simply summed up as shown in (24) and (25). In the future work, different user weights can be introduced into the expression of γ_E.

$\mathbf{E}$ and $\mathbf{C}$ are two Hermitian matrices as can be seen from (25). The optimization problem in (26) can be solved as a classical eigenvalue problem [10], [11]. The eigenvalue decomposition of $\mathbf{C}$ is shown as

$$\mathbf{C} = \mathbf{U}_C\mathbf{D}_C\mathbf{U}_C^H \tag{27}$$

where $\mathbf{U}_C$ is constructed of the eigenvectors of $\mathbf{C}$, and $\mathbf{D}_C$ is a diagonal matrix with descendingly sorted eigenvalues. An assistant matrix $\mathbf{Q}$ is defined as

$$\mathbf{Q} = \left(\mathbf{U}_C\mathbf{D}_C^{-\frac{1}{2}}\right)^H\mathbf{E}\left(\mathbf{U}_C\mathbf{D}_C^{-\frac{1}{2}}\right). \tag{28}$$

The range of γ_E is determined by the eigenvalues of $\mathbf{Q}$

$$\lambda_{Q,\min} \leq \gamma_E = \frac{\mathbf{p}^T\mathbf{E}\mathbf{p}^*}{\mathbf{p}^T\mathbf{C}\mathbf{p}^*} \leq \lambda_{Q,\max} \tag{29}$$

where $\lambda_{Q,\min}$ and $\lambda_{Q,\max}$ are the minimum and maximum eigenvalues of $\mathbf{Q}$, respectively. The precoder that maximizes γ_E can be written as

$$\mathbf{p}_H = \underset{\|\mathbf{p}\|_F^2 = E_R}{\arg\max}\, \gamma_E = \mu \mathbf{U}_C^* \mathbf{D}_C^{-1/2} [\mathbf{U}_Q(:,1)]^* \tag{30}$$

where μ is the normalization coefficient satisfying $\|\mathbf{p}_H\|_F^2 = E_R$, and $\mathbf{U}_Q(:,1)$ is the eigenvector of $\mathbf{Q}$ relative to $\lambda_{Q,\max}$.

Usually, the optimization problems defined in (22) and (23) cannot be solved exactly, and there is no closed-form expression for the precoders. Some iterative methods can be employed, but the complexity is remarkably higher compared with the solution in (30).

Simulation results in Section V demonstrate that the proposed distributed precoder apparently outperforms the fixed AF protocol. Compared with the precoders optimizing the system capacity or reliability in (22) and (23), the proposed distributed precoder in (30) has a closed-form expression and is able to provide performance close to optimum in terms of both outage probability and ergodic capacity. The proposed distributed precoder is a design trade-off between the system capacity and reliability in the multi-user system.

IV. Joint Precoding Design

In Section III, the design of $\mathbf{p}$ is presented without the consideration of $\mathbf{F}$ at S. However, replacing $\mathbf{H}$ with $\mathbf{HF}$, the design in (30) can also be used. The design of $\mathbf{F}$ in cooperation with $\mathbf{p}$ is considered in this section.

A. SLNR Maximization

If the distributed precoding vector is constrained by $\|\mathbf{p}\|_F^2 = 1$, the maximum received target signal power at D_j is $\|\mathbf{e}_j\|_F^2$ when $\mathbf{p} = \mathbf{e}_j^*/\|\mathbf{e}_j\|_F$. Similarly, the equivalent channel vector of the interference from d_j to D_k is $\mathbf{c}_{jk}$, $j \neq k$ as shown in (16). This also implies that the maximum received interference power at D_k from d_j is $\|\mathbf{c}_{jk}\|_F^2$ ($\mathbf{p} = \mathbf{c}_{jk}^*/\|\mathbf{c}_{jk}\|_F$). Therefore, the *maximum* SLNR of the jth data stream can be defined as

$$\gamma_{M,j} = \frac{E_R \|\mathbf{e}_j\|_F^2}{E_R \sum\limits_{k,k\neq j} \|\mathbf{c}_{jk}\|_F^2 + \sigma^2} \tag{31}$$

where the "$\sum$" term in the denominator is the interference power experienced at other destination nodes leaking from d_j. The definition in (31) is based on the maximum received signal and maximum interference power as mentioned above. Therefore, it is termed the *maximum* SLNR.

The *maximum* SLNR defined in (31) can be written as a function of the precoding vector $\mathbf{f}_j = \mathbf{F}(:,j)$. It is required that $\|\mathbf{F}\|_F^2 = E_S$ due to the power constraint of S. In addition, it is assumed that the columns of $\mathbf{F}$ ($\mathbf{f}_j$) have the same Frobenius norm, i.e., $\|\mathbf{f}_j\|_F^2 = E_S/N_D$.

Considering multi-user precoding at S, (15) can be rewritten as

$$\mathbf{e}_j = \mathbf{H}_{G,j}\mathbf{f}_j \tag{32}$$

where

$$\mathbf{H}_{G,j} = \mathrm{diag}\left[\mathbf{G}_a(j,:)\right]\mathbf{H}. \tag{33}$$

Similarly,

$$\mathbf{c}_{jk} = \mathbf{H}_{G,k}\mathbf{f}_j. \tag{34}$$

According to the Frobenious norm constraint of the precoding vectors, the noise power in the denominator of (31) can be replaced with $\mathbf{f}_j^H(N_D/E_S \cdot \sigma^2 \cdot \mathbf{I}_{N_S})\mathbf{f}_j$. The *maximum* SLNR is thus rewritten as

$$\begin{aligned}\gamma_{M,j} &= \frac{\mathbf{f}_j^H \mathbf{H}_{G,j}^H \mathbf{H}_{G,j}\mathbf{f}_j}{\sum\limits_{k,k\neq j} \mathbf{f}_j^H \mathbf{H}_{G,k}^H \mathbf{H}_{G,k}\mathbf{f}_j + \sigma^2} \\ &= \frac{\mathbf{f}_j^H \mathbf{H}_{G,j}^H \mathbf{H}_{G,j}\mathbf{f}_j}{\mathbf{f}_j^H \left[\sum\limits_{k,k\neq j}\left(\mathbf{H}_{G,k}^H\mathbf{H}_{G,k}\right) + \frac{N_D\sigma^2}{E_S}\mathbf{I}_{N_S}\right]\mathbf{f}_j}.\end{aligned} \tag{35}$$

Note that $\mathbf{e}_j$ and $\mathbf{c}_{jk}$ are quite similar as can be observed in (32) and (34). The difference lies in the corresponding rows of $\mathbf{G}_a$. The multi-user precoding design at S should take the interference signal power into account. If each precoding vector is designed to maximize the target signal power, the interference power will also be enhanced due to the similarity between $\mathbf{e}_j$ and $\mathbf{c}_{jk}$. The *maximum* SLNR defined in (31) includes the target signal and leakage interference powers. Furthermore, the precoding design is easier since $\gamma_{M,j}$ is a function of $\mathbf{f}_j$ and independent of the other columns of $\mathbf{F}$.

The fraction expression of (35) is similar to (24), so that the classical solution in (28)-(30) can be extended to achieve the initial multi-user precoding vectors as follows

$$\mathbf{f}_j = \underset{\mathbf{f}_j}{\arg\max}\, \gamma_{M,j} = \mu \mathbf{U}_{C_L}\mathbf{D}_{C_L}^{-1/2}\mathbf{U}_{Q_L}(:,1) \tag{36}$$

where $j \in \{1,2,\cdots,N_D\}$, μ is the normalization coefficient, $\mathbf{U}_{C_L}$ and $\mathbf{D}_{C_L}$ can be obtained by the eigenvalue decomposition of $\mathbf{C}_L$

$$\mathbf{C}_L = \sum_{k,k\neq j}\left(\mathbf{H}_{G,k}^H\mathbf{H}_{G,k}\right) + \frac{N_D\sigma^2}{E_S}\mathbf{I}_{N_S} = \mathbf{U}_{C_L}\mathbf{D}_{C_L}\mathbf{U}_{C_L}^H, \tag{37}$$

and $\mathbf{U}_{Q_L}(:,1)$ is the eigenvector of the largest eigenvalue of $\mathbf{Q}_L$

$$\mathbf{Q}_L = \left(\mathbf{U}_{C_L}\mathbf{D}_{C_L}^{-\frac{1}{2}}\right)^H \mathbf{H}_{G,j}^H\mathbf{H}_{G,j}\left(\mathbf{U}_{C_L}\mathbf{D}_{C_L}^{-\frac{1}{2}}\right). \tag{38}$$

B. Channel Similarity

In (31)-(38), the initial multi-user precoding matrix $\mathbf{F}$ ($\mathbf{f}_j$) is designed to maximize the *maximum* SLNR defined in (31). However, the *maximum* SLNR is calculated with the maximum signal power and maximum interference power. The distributed precoding vector $\mathbf{p}$ determines the real values of the signal and interference power at all the destination nodes. Generally speaking, a distributed precoder cannot maximize SINRs of N_D users simultaneously. $\mathbf{p}_H$ designed in (30) is a trade-off among the optimum precoding vectors for every destination node since the hybrid SINR defined in (24) takes into account equivalent target signal and interference channels of all the users. If the equivalent target signal channels of several users are similar, e.g., the angle between any two channel vectors is close to 0, i.e.,

$$\frac{\left|\mathbf{e}_j^H\mathbf{e}_k\right|}{\|\mathbf{e}_j\|_F\,\|\mathbf{e}_k\|_F} \to 1, j \neq k, \tag{39}$$

$\mathbf{p}_H$ can approximately maximize the received SINRs at all the destination nodes. The similarity among the equivalent channels can be used to improve on system performance.

On the other hand, the equivalent channels are affected by $\mathbf{F}$. Therefore, we can divide the N_D users into two groups, i.e., the interference mitigation group and channel similarity group. The precoding vectors at S of the interference mitigation group are designed to maximize the *maximum* SLNR as described in (36)-(38). The ones of the channel similarity group are designed to guarantee the channel similarity among all the equivalent channels. It is intuitive that the performance of the users in the first group are worse than that of those in the second group if random grouping or fixed group division is used. Adaptive group division should be adopted. The users with better channel qualities are selected into the interference mitigation group.

The initial multi-user precoding matrix $\mathbf{F}$ is calculated to maximize the *maximum* SLNR. Then the equivalent channels $\mathbf{e}_j, j \in \{1, 2, \cdots, N_D\}$ are calculated using (32). The Frobenius norms of all the equivalent channels are calculated and sorted, and the first $\lfloor N_D/2\rfloor$ users with the largest Frobenius norms are chosen into the interference mitigation group. It can be assumed without loss of generality that the 1st - $\lfloor N_D/2\rfloor$th users are chosen. Then, the precoding vectors of the channel similarity group ($\mathbf{f}_j, \lfloor N_D/2\rfloor + 1 \leq j \leq N_D$) are designed to guarantee the similarity between $\mathbf{e}_1 \sim \mathbf{e}_{\lfloor N_D/2\rfloor}$ and $\mathbf{e}_{\lfloor N_D/2\rfloor+1} \sim \mathbf{e}_{N_D}$. Each precoding vector is calculated independently as follows

$$\begin{aligned}\mathbf{f}_j &= \underset{\|\mathbf{f}_j\|_F^2 = E_S/N_D}{\arg\max} \sum_{k=1}^{\lfloor N_D/2\rfloor} \left|\mathbf{e}_j^H\mathbf{e}_k\right|^2 \\ &= \mu\mathbf{H}_{G,j}^H\mathbf{U}_{E_{\lfloor N_D/2\rfloor}}(:,1).\end{aligned} \tag{40}$$

where $\mathbf{U}_{E_{\lfloor N_D/2\rfloor}}(:,1)$ is the eigenvector of the largest eigenvalue of $\mathbf{E}_{\lfloor N_D/2\rfloor}$

$$\mathbf{E}_{\lfloor N_D/2\rfloor} = \sum_{j=1}^{\lfloor N_D/2\rfloor} \mathbf{e}_j\mathbf{e}_j^H = \mathbf{U}_{E_{\lfloor N_D/2\rfloor}}\mathbf{D}_{E_{\lfloor N_D/2\rfloor}}\mathbf{U}_{E_{\lfloor N_D/2\rfloor}}^H. \tag{41}$$

The relationship between the two groups can be seen clearly from a special case of $N_D = 2$. Equation (40) can be simplified as

$$\mathbf{f}_2 = \mu\mathbf{H}_{G,2}^H\mathbf{H}_{G,1}\mathbf{f}_1. \tag{42}$$

That is, the equivalent channels of the two users are the same without considering the Frobenious norm. With adaptive grouping, the performance of all the users are identical.

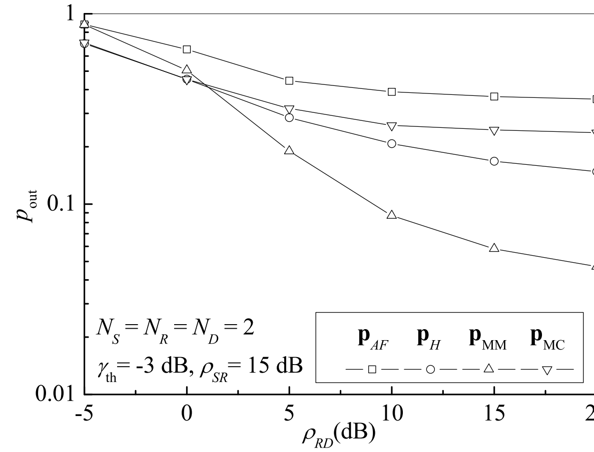

Fig. 2. Distributed precoding through relay nodes: outage probability.

V. Numerical and Simulation Results

Independent and identically distributed Rayleigh fading channels are assumed, i.e., $\mathbf{H}(i,k) \sim \mathcal{CN}(0, \sigma_{SR}^2)$, $\mathbf{G}(j,i) \sim \mathcal{CN}(0, \sigma_{RD}^2)$, $k \in \{1, 2, \cdots, N_S\}$, $i \in \{1, 2, \cdots, N_R\}$, and $j \in \{1, 2, \cdots, N_D\}$. $E_S = N_D$, $E_R = 1$, $\sigma^2 = 1$. The average signal-to-noise ratios (SNRs) of the two phases are defined as $\rho_{SR} = E_S\sigma_{SR}^2/\sigma^2$, $\rho_{RD} = E_R\sigma_{RD}^2/\sigma^2$.

Two evaluation metrics are considered, i.e., the ergodic capacity

$$C = \sum_{j=1}^{N_D} \log_2(1 + \gamma_j), \tag{43}$$

and the outage probability

$$p_{\text{out}} = \frac{1}{N_D}\sum_{j=1}^{N_D} \Pr(\gamma_j < \gamma_{\text{th}}) \tag{44}$$

where γ_{th} is the SNR threshold.

Firstly, distributed precoding through N_R relay nodes is evaluated as shown in Figs. 2 and 3. The three precoders described in Section III [(30), (22) and (23)] are compared. Moreover, the simple AF relaying scheme without adaptation $\mathbf{p}_{AF} = \sqrt{E_R/N_R}\,[1, 1, \cdots, 1]^T$ is also used as a comparison. The two precoders in (22) and (23) are achieved with exhaustive search through the unitary space.

As shown in Fig. 2, the outage probability curves of the four precoders exhibit the so-called “floor”, since ISI cannot be completely eliminated with a small number of relay nodes. It is intuitive that $\mathbf{p}_{\text{MM}}$ in (23) is best if ρ_{RD} is large enough. $\mathbf{p}_H$ performs close to $\mathbf{p}_{\text{MM}}$ and outperforms it when $\rho_{RD} < 1$ dB. With $\mathbf{p}_{AF}$, signals from relay nodes are randomly combined at each destination node, so that $\mathbf{p}_{AF}$ gives the worst performance.

Fig. 3 compares the ergodic capacities of the four distributed precoders. $\mathbf{p}_{\text{MC}}$ outperforms other precoders, which is different from the result in Fig. 2. $\mathbf{p}_{AF}$ is still the worst one due to non-coherent combination. The ergodic capacity of $\mathbf{p}_H$ is close to that of $\mathbf{p}_{\text{MC}}$ and larger than those of the other precoders. The proposed $\mathbf{p}_H$ is a trade-off between $\mathbf{p}_{\text{MC}}$ and $\mathbf{p}_{\text{MM}}$ as shown in Figs. 2 and 3, i.e., a trade-off between reliability

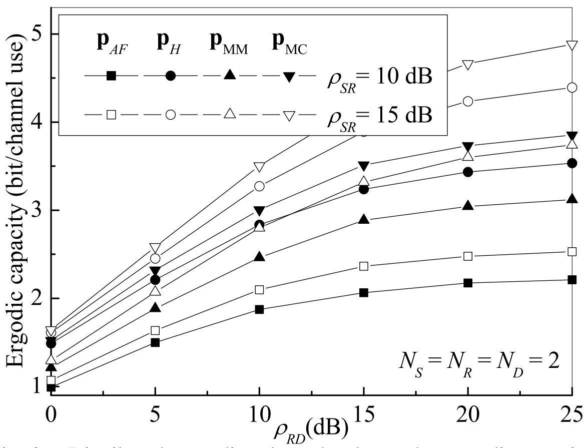

Fig. 3. Distributed precoding through relay nodes: ergodic capacity.

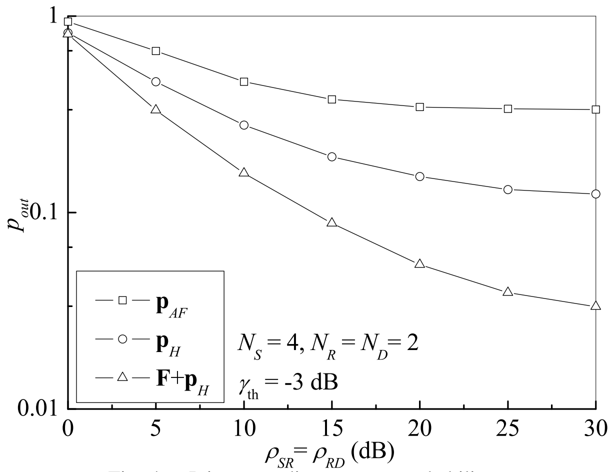

Fig. 4. Joint precoding: outage probability.

and capacity. Additionally, $\mathbf{p}_H$ has a closed-form expression as shown in (30), which is an evident advantage and different from the designs in (22) and (23).

Then, the joint design of multi-user precoding at S and distributed precoding through N_R relay nodes in Section IV is evaluated in Figs. 4 and 5. The fixed distributed precoding vector $\mathbf{p}_{AF}$ is also used as a comparison. The legend "$\mathbf{p}_H$" in the two figures denotes the distributed precoding vector in (30). If the distributed precoder is used without the cooperation of the multi-user precoder at S, N_D antennas at S are randomly selected for transmission, which is equivalent to $\mathbf{F} = [\mathbf{I}_{N_D}, \mathbf{0}_{N_D,N_S-N_D}]^T$. Fig. 4 gives the outage probability performance of distributed precoding as well as joint precoding. The distributed precoder $\mathbf{p}_H$ outperforms the fixed precoder $\mathbf{p}_{AF}$, and the cooperation of the multi-user precoding matrix $\mathbf{F}$ further improves on the system reliability. Similar conclusions can be drawn from Fig. 5. The advantage of joint precoding in Section IV is very apparent at high SNRs ($\rho_{SR} = \rho_{RD} > 15$ dB).

VI. Conclusion

Multi-user precoders, i.e., the multi-user precoder at the source node and the distributed precoder through relay nodes, in the multi-relay system is investigated. The trade-off among

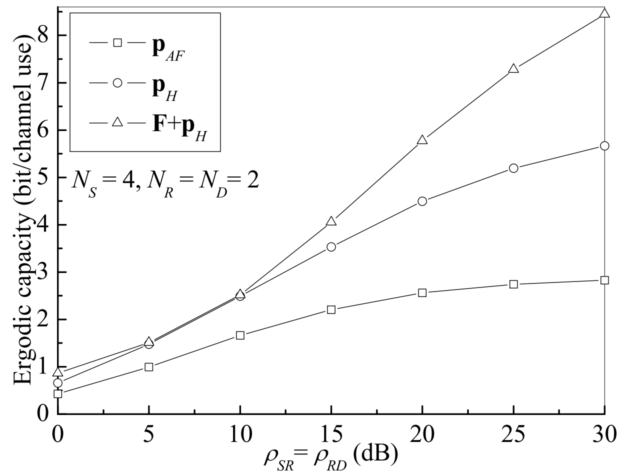

Fig. 5. Joint precoding: ergodic capacity.

multiple users is considered in the precoding design, as well as the trade-off between system reliability and capacity. A hybrid SINR is defined and the closed-form expression for the distributed precoder is derived. Then, we investigate the joint design of the two precoders. The users are adaptively divided into two groups. The precoding vectors of the first group are designed to enhance the received signal power and mitigate the leakage interference to other users. The precoding vectors of the second group are designed to guarantee that the distributed precoding vector can enhance the SINR of each user simultaneously. The joint precoding is preferred for the high SNR region when a large number of antennas are equipped at the source node.

References

[1] C. B. Chae, T. Tang, R.W. Heath Jr., and S. Cho, "MIMO relaying with linear processing for multiuser transmission in fixed relay networks," *IEEE Trans. Signal Processing*, vol. 56, no. 2, pp. 727-738, Feb. 2008.

[2] R. Zhang, C.C. Chai, and Y.C. Liang, "Joint beamforming and power control for multiantenna relay broadcast channel with QoS constraints," *IEEE Trans. Signal Processing*, vol. 57, no. 2, pp. 726-737, Feb. 2009.

[3] N. Devroye, N.B. Mehta, and A.F. Molisch, "Asymmetric cooperation among relays with linear precoding," in *Proc. IEEE Globecom 2007*, Washington DC., Nov. 2007, pp. 4391-4396.

[4] G. Atia and A.F. Molisch, "Cooperative relaying with imperfect channel state information," in *Proc. IEEE Globecom 2008*, New Orleans, Nov. 2008, pp. 1-6.

[5] N. Devroye, N.B. Mehta, and A.F. Molisch, "Asymmetric cooperation among wireless relays with linear precoding," *IEEE Trans. Wireless Communications*, vol. 7, no. 12, part 2, pp. 5420-5430, Dec. 2008.

[6] J. Zhao, M. Kuhn, A. Wittneben, and G. Bauch, "Cooperative transmission schemes for decode-and-forward relaying," in *Proc. IEEE PIMRC 2007*, Athens, Greece, Sept. 2007, pp. 1-5.

[7] Y. Zheng and S. Blostein, "Downlink distributed beamforming through relay networks," in *Proc. IEEE Globecom 2009*, Honolulu, Hawaii, USA, Dec. 2009, pp. 1-6.

[8] H. Long, F. Wang, Y. Zhang, K. Zheng, and W. Wang, "Successive phase sharing and distributed multi-user precoding in multi-relay systems," *IEEE Signal Processing Letters*, vol. 17, no. 10, pp. 859-862, Oct. 2010.

[9] Y. Zheng and S. Blostein, "Optimization of power constrained multi-source uplink relay networks," in *Proc. IEEE Globecom 2009*, Honolulu, Hawaii, Dec. 2009, pp. 1-6.

[10] K.K. Wong, R.D. Murch, and K.B. Letaief, "Performance enhancement of multiuser MIMO wireless communication systems," *IEEE Trans. Comms.*, vol. 50, no. 12, pp. 1960-1970, 2002.

[11] K.K. Wong, R.D. Murch, and K.B. Letaief, "Orthogonal space division multiplexing through joint use of multi-user MIMO smart antennas," in *Proc. PIMRC 2002*, Lisbon, Portugal, Sept. 2002, pp. 577-581.